A LARGE SOLID ANGLE SUPERCONDUCTING IRONLESS MAGNET FOR THE DESY STORAGE RINGS

H.J. Besch and U. Trinks
Physikalisches Institut der Universität Bonn
Bonn, West Germany

Abstract

For the DESY storage rings a superconducting magnet for a large solid angle magnetic detector is under construction. The magnet consists of 8 identical nearly rectangular ironless coils, which are arranged like butterfly wings around the beam at the interaction point to produce a circular field decreasing very rapidly near the beam and outside thus requiring no magnetic shielding. Each coil is contained in its own cryostat and carries a current of 1.2×10^6 A in a cross section of 176 cm^2. The magnet covers polar angles between 40 and 140 degrees providing a solid angle of 7.3 sr. The integrated field length is 19 kG·m. The total length is 4 m, the free inner diameter is 1.3 m and the total diameter is 5.5 m. As the current density is very high, one test coil will be set up first. A magnet of this type may be useful also for large solid angle spectrometers connected with a tagged photon beam.

I. Introduction

A superconducting ironless magnet is planned[1] for experiments at the DESY storage rings in Hamburg. It will have the following properties:

Acceptance:	azimuthal angle	$0.75 \times 2\pi$
	polar angle	40-140
	solid angle	7.3 sr
Integrated field length		19 kG·m
Residual field		
at beam position		< 10 G
in a distance of 4.5 m from the beam		< 10 G

After a general view of the construction the properties of the field and the particle trajectories are given. After that some details about the mechanical construction are described. Finally some notes are given about the conductor, the coils and the cooling system.

An overall view is given in Fig. 1. Eight identical plates are arranged rotationally symmetrically around the beam axis. The diameter $2 \times R_i$ of the free inner region can be changed by substituting the supporting rings, thus giving a high degree of flexibility. Cross sections (longitudinal and vertical) are shown in Fig. 2. The dimensions are given in Table I. To get large acceptances the plates taper off at the beamside edge. Each plate forms a box representing a cryostat. The superconducting coils are suspended in the boxes, the dimensions of which are contained in Fig. 3 and Table I.

Between the plates the current in the coils produces an almost concentric magnetic field around the beam axis. The field decreases very

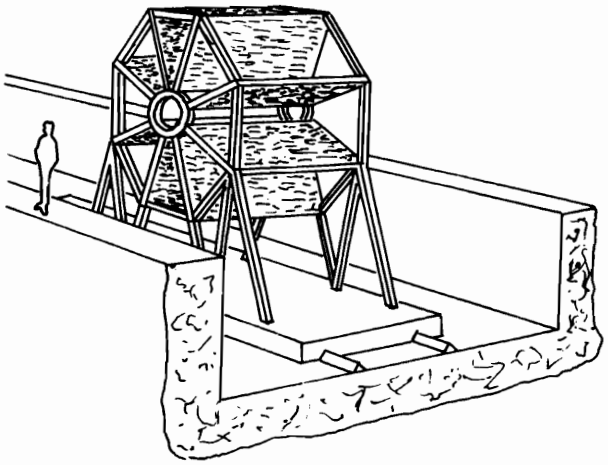

Fig. 1. Overall view of the magnet.

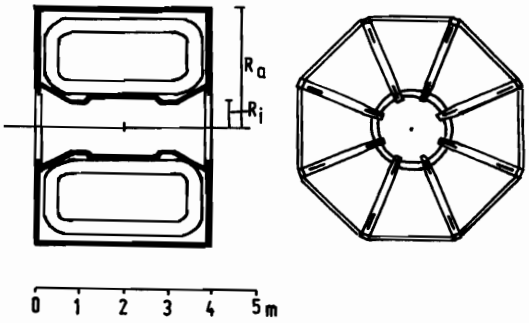

Fig. 2. Cross sections (longitudinal and vertical).

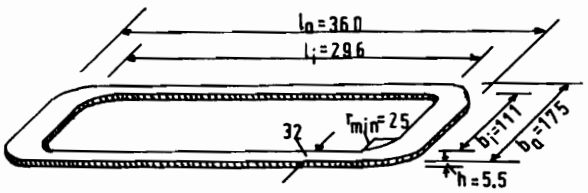

Fig. 3. The coil.

TABLE I. Geometric Dimensions

Plate:	height	D	= 20.5 cm
	height at the inner edge	D′	= 12 cm
	length	L	= 400 cm
	width	B	= 210 cm
Coil:	outside	l_a	= 360 cm
		b_a	= 175 cm
	inside	l_i	= 296 cm
		b_i	= 111 cm
	height	h	= 5.5 cm
	min. curvature radius	r_{min}	= 25 cm
Weights:	coil packet	P_c	= 2.5 ton
	plate	P^p	= 7.6 ton
	magnet	P^p	= 65 ton

fast in the neighbourhood of the beams as well as outside the magnet. Particles starting from the interaction region move essentially in planes containing the beam axis.

TABLE II. Properties for Different R_i

Version	I	II	III	x
Inner radius R_i	40	65	90	cm
Outer radius R_a	250	275	300	cm
Azimuthal angle	0.61	0.75	0.80	2π
Polar angle	32-148	39-141	45-135	[°]
Solid angle	6.5	7.3	7.1	sr
Current per coil		1.2×10^6		A
Current density J		6.8×10^3		A/cm^2
Field length $\int Bdr$	22.7	19.0	16.7	kG·m
Stored energy	40.4	37.8	37.0	MJ
Max. field at the superconductor	42	40	37	kG

Table II contains a summary of the acceptances and the field properties for different inner radii R_i and constant currents of $I = 1.2 \times 10^6$ A per coil. There are several reasons preventing one from enlarging the currents in favour of a higher field length $\int Bdr$:

a) The current density is rather large in relation to the stored magnetic energy.[2] Because of the limited space it is not possible to enlarge the cross section of the coil. Moreover, the ratio of superconductor to copper should not be enlarged (see below). Finally, stronger forces on the conductor itself may destroy it.

b) Stronger overall forces would require more space for supporting constructions thus restricting the acceptance.

c) The maximum field at the superconductor would increase.

In Table II the geometrical angle acceptances given by the mechanical dimensions of the plates are quoted.

In the following all calculations are made for the smallest inner diameter of 2×40 cm providing maximum forces and fields.

II. The Field

The magnet is ironless. Therefore it is easy to calculate the field. No measurements will be needed, if the field has to be adapted to the experimental requirements.

To describe the field we use cylindrical coordinates. z is the magnet axis (z= 0 at the interaction point), r means the radial direction, and φ is the azimuthal angle with $\varphi = 0$ in the middle of two plates. The field component B_φ is the most important one for momentum analysis. B_z and B_r are of importance only near the coils. A cross section of the field distribution B is given in Fig. 4 (at z = 0).

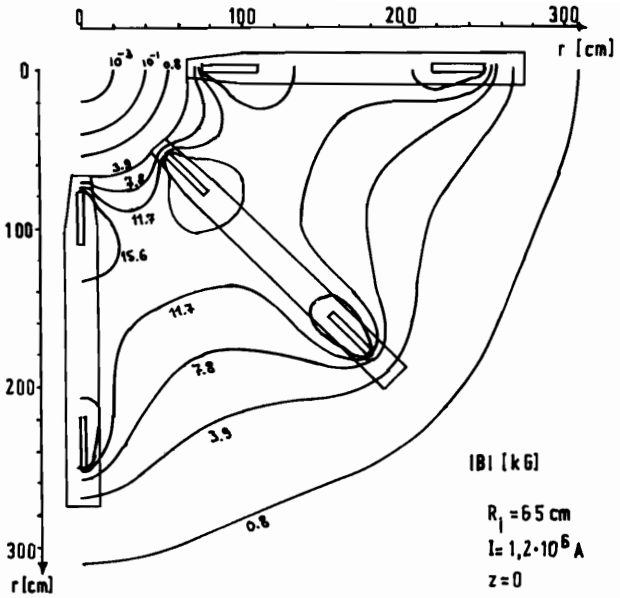

Fig. 4. Cross section of the field B.

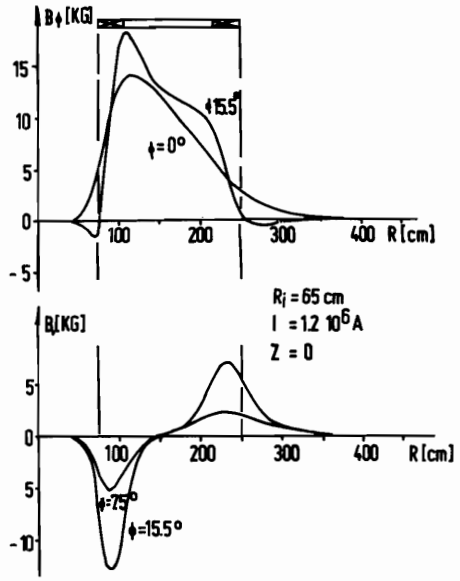

Fig. 5. The field components $B_\varphi(r)$ and $B_r(r)$.

Figure 5 shows the components $B_\varphi(r)$ and $B_r(r)$ along radial lines for different angles φ. $B_\varphi(r)$ is almost triangularly shaped, the maximum slightly shifted to the magnet axis. $B_r(r)$ disappears at $\varphi = 0$ and changes sign as φ turns from negative to positive values.

Because of the fast decreasing field strength near the magnet axis the beams pass the magnet without being influenced. In a distance of r = 20 cm from the magnet axis the field is B < 1 G if the coils are perfectly symmetrically adjusted (for R_i = 65 cm). A radial or azimuthal displacement Δs of one coil causes a variation of the residual field

$$\Delta B \leq 10 \times \Delta s \quad (G/mm)$$

Therefore construction and adjusting tolerances of $\Delta s \leq 1$ mm are allowed. Outside the magnet the field also decreases rapidly.

III. The Trajectories and Acceptances

In the following only particles of one sign of charge are considered. Figure 6 shows particle trajectories for different momenta and polar angles ($\varphi = 0$). The bending angles are given in Fig. 7 as functions of the polar angle θ. In Fig. 8 is plotted the azimuthal acceptance in dependence on the polar angle for several momenta. The geometrical azimuthal acceptance represented by the solid

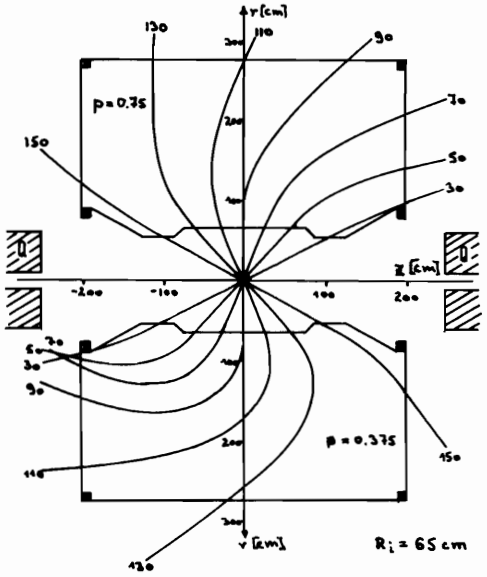

Fig. 6. Particle trajectories for p = 375 (down) and p = 750 MeV/c (up). R_i = 65 cm, I = 1.2 $\times$ 10^6 A.

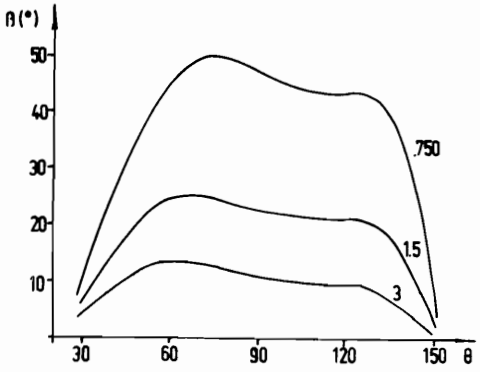

Fig. 7. The bending angles $\beta(\theta)$.

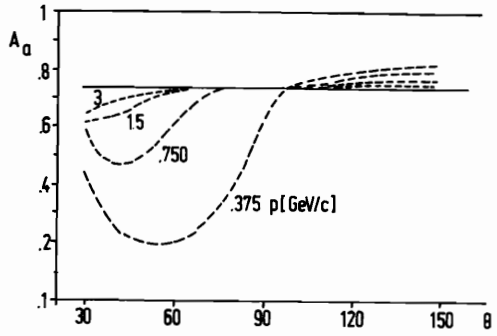

Fig. 8. The azimuthal acceptance $A_a(\theta)$.

line is given by the plate dimensions. It is modified by the radial field component B_r (and slightly by B_z): particles starting with a polar angle $\theta = 90^o$ enter the magnet in radial direction, hence there is nearly no influence of B_r. Particles with $\theta > 90^o$ will be deflected from the regions near the plates to the middle between two plates. Here we have a focusing effect, so that the real acceptance slightly exceeds the geometrical limit. On the other hand particles with $\theta < 90^o$ are defocussed by B_r and B_z so that they may hit the plates before leaving the magnet at the outer edges or at the faces.

IV. The Mechanical Construction

Because of the high currents the forces are rather strong. First we discuss the forces caused by currents parallel to the magnet axis and then those from the perpendicular ones. The main forces are listed in Table III.

TABLE III. The Forces

P	= 300 ton	
P_i	= 500 ton	(R_i = 40 cm, I = 1.2 $\times$ 10^6 A)
$P_a = P_d$	= 200 ton	
P_s	= 90 ton	
Q_i	= 0.27 ton/mm displacement	
Q_a	= 0.165 ton/mm displacement	

The parallel inner parts of the coils are attracted to the central axis by P_i. The outer parts with the opposite current pull with weaker forces P_a in the opposite direction, so that the resulting force $P = P_i - P_a$ on each plate is directed to the axis. P_d is the force pulling apart the outer segment of one coil from the inner one. P_d is equal to the smaller one of P_i and P_a, so $P_d = P_a$.

With respect to the azimuthal forces caused by azimuthal displacements the system is in a state of unstable equilibrium. The azimuthal displacement of one coil gives rise to the forces Q_i and Q_a which act on the inner and outer parts of the coil respectively. The mechanical construction can sustain forces caused by displacements up to 10 mm.

With respect to displacements in the z-direction the system is stable. P_s is the force on the coil parts perpendicular to the magnet axis.

After this survey of the forces we describe the construction of one plate. The coil is enclosed in a rectangular steel blanket thus giving stability. The blanket consists of two rings, which are connected by bolts and made tight by welding (see Fig. 9). The coil is held together against the repulsive forces P_d and P_s by two steel panels inside the frame. The panels (each 1.5 cm thick) have a distance of 6 cm. They are pierced to give space for the connecting elements between the cold coil packet and the warm walls of the vacuum chamber. The vacuum chamber forms a flat box with an inner free space of about $200 \times 14.5 \times 377$ cm^3. It contains the cold coil packet with the outer dimensions of about $185 \times 9.5 \times 372$ cm^3. Thus nearly everywhere there remains a distance of 2.5 cm filled with super-insulation.

The large surfaces of the vacuum chamber have to be supported against the atmospheric pressure. This is done by several rods from one cover to the other inside the box. In the middle there are several blocks aligned. The supporting elements leading the radial forces P from the coil packet to the vacuum chamber are tied at one end in these blocks and at the other in either panel of the coil packet. Each of the twelve supporting

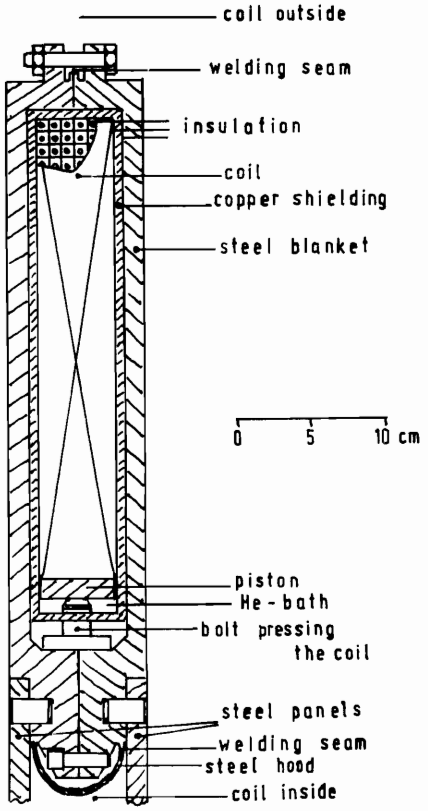

Fig. 9. The coil enclosed in the steel blanket.

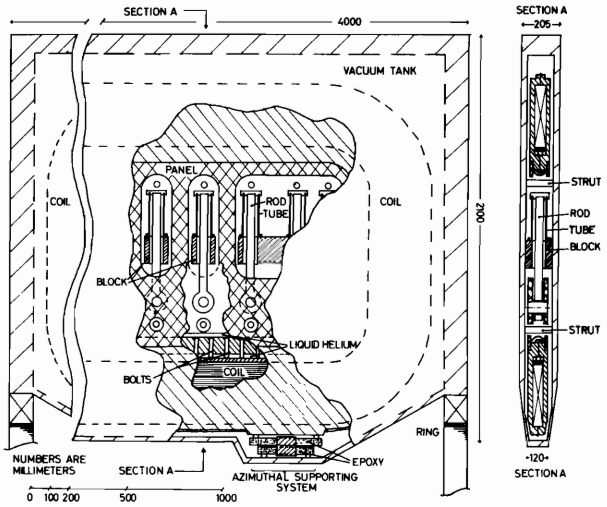

Fig. 10. The construction of a plate.

elements consists of a system of a rod and a tube of titanium (cross section 12.5 cm^2, total free length 57 cm). Titanium has a very small thermal conductivity at low temperatures (4-80°K: 2.2 W/cm) and a high tensile strength (100 kg/mm^2). The length of each rod-tube system is adjustable to provide uniform load. The flux is led from the blocks across the covers of the vacuum chamber to the inner supporting rings at the faces of the magnet. These rings are placed under the radial beams forming the vacuum chamber frame (see Fig. 10). Calculation gives maximum stresses of 1.1 kg/mm^2 in the chamber covers (steel).

The coil packet is held in azimuthal direction by four clamps positioned at its edges. Because of the smaller azimuthal forces these clamps consist mainly of epoxy. The outer rings at the magnet faces have to sustain the azimuthal forces. They are made of tubes containing the helium pipes and conductors connecting one plate to the next.

V. The Coils

Each coil consists of three identical pancakes and has $6 \times 35 = 210$ turns of a hollow composite conductor of a cross section of 8×8 mm^2 connected electrically in series, for the cooling system in parallel (see Fig. 11). This is done

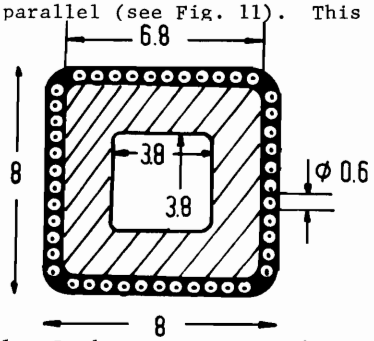

Fig. 11. Conductor cross section.

by use of Morpurgo-type insulators. The conductor will have to carry a current of 5700 A. It is composed from a hollow rectangular copper pipe and 44 multifilament superconductors, which are twisted and soft-soldered around the pipe. As the maximum field at the conductor will be 42 kG the conductor (with an adequate safety margin) is specified to carry a current of 8000 A in a transversal field of 48 kG at 5 K. The copper resistivity has to be less than 1.5×10^{-8} Ω·cm.

Mechanical stresses are caused by magnetic and thermal forces, especially during the cooling down period. With a properly adjusted cooling down time it is possible to keep the mechanical stresses below 900 kg/cm^2.

TABLE IV. The Coil

Current per conductor	5700 A
Number of turns	210
Mean length of one turn	10 m
Cross section	8 x 8 mm^2
Inner cross section of the cooling pipe	3.8 x 3.8 mm^2
Ratio of superconductor to copper	1 / 5.3

VI. Cooling

As it is impossible by reasons of space to use a nitrogen-cooled radiation shielding, a quite high cooling power is required because of the large surface area. The radiation losses can be reduced by superinsulation (20 mm) to 1.5-2 W/m^2. The losses through the titanium rods and azimuthal supporting system will be (as nitrogen cooling will be used there) only 100 W. Together with various losses of 50 W this adds up to a total thermal loss of 400 W. The magnet needs four current leads, because it can be divided into two parts. These leads will have a consumption of 1.7 g/sec liquid helium, together.

The refrigerator thus — again with an adequate safety margin — will have to supply simultaneously

at 80 K 2500 W
at 4.2 K 600 W
and 2.8 g/sec liquid helium.

The helium flow diagram is shown in Fig. 12. In stationary operation the valves V2, V3, V5, V6, V7, V11,...V18 will be closed, the others will be open. After having passed through the J.T. valve V1 and the auxiliary cryostat — filled with liquid helium — the helium is fed at 10 kg/cm^2 and 4.2 K into 8 coil plates CC1...CC8 connected in parallel. In each coil plate this supercritical helium divides into the three double pancakes and flows through the hollow conductor, expanding is enthalpic to about 8 kg/cm^2 and warming up about 0.2 K. In the J.T. valves V21...V28 the helium expands to low pressure. The resulting mixture of gaseous and liquid helium is collected in the coil cryostats, cooling the copper shielding very effectively by boiling. The vapour and unused liquid are passed to the auxiliary cryostat, cooling down there the helium emerging at high pressure and temperature from the refrigerator.

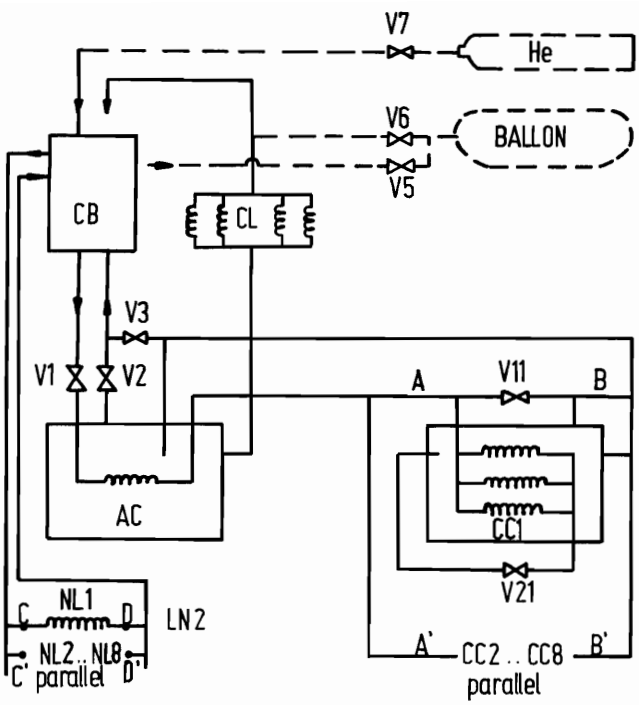

Fig. 12. The helium flow diagram.

Heat sources should not be present in an intrinsically stable conductor. In spite of this it has shown up, that it is impossible to build large coils cooled by heat conduction. The hybrid cooling system used here allows to carry away a large amount of locally generated heat, because there exist no bubbles in the conductor, the heat transfer coefficient will be as large as 0.17 W/cm^2 K and the helium flow velocity is quite high. On the other hand by bath cooling the copper shielding is held at constant temperature.

VII. Quenching

If the magnet, whatever the reasons may be, will quench, the stored energy of 40 MJ will have to disappear in a short time. An external shunt resistor, the resistance of which will be 50 mΩ at 300 K, will take up a considerable amount of the stored energy, as the resistance of the copper of one coil is about 6 mΩ below 30 K. By adjusting the temperature coefficient of the resistivity and the heat capacity of the shunt resistor, it is possible to keep the ratio of the shunt and inner resistance nearly constant during discharge. The coils will warm up to 59...73 K, depending on the number of coils following the quenching of the first one. This causes only negligible thermal stresses. Voltages to ground were roughly calculated and have shown to be less than 350 V. The magnet will discharge in this case in some 20 to 30 sec.

Acknowledgements

We are greatly indebted to Mr. M. Morpurgo, CERN, without whose invaluable help it would not have been possible for us to develop this project. We would also like to express our acknowledgements to Mr. Eschricht, Ganske, Horlitz, Knust and Wolff from DESY.

References

1. H.J. Besch and U. Trinks, "Vorschlag zur Realisierung des Oktopusmagneten für den DESY-Speicherring," Physikalisches Institut der Universität Bonn Report PIB 1-180 (Juni 1972).

2. M.S. Lubell et al., Oak Ridge National Laboratory Report ORNL-TM-3404 (June 1971).

3. M. Morpurgo, Particle Accelerators 1, 255 (1970).